8th Power Electronics, Drive Systems & Technologies Conference (PEDSTC 2017)
14-16 Feb. 2017, Ferdowsi University of Mashhad, Mashhad, Iran

# Analytical Modeling and Simulation of Overexcitation Process in Hysteresis Motor

AmirHossein PirZadeh Abolfazl Halvaei Niasar Sayyed Hossein Edjtahed
Department of Electrical & Computer Engineering, University of Kashan, Kashan, P.O.Box: 87317-53153, Iran
a.pirzadeh@grad.kashanu.ac.ir halvaei@kashanu.ac.ir ejtahed@kashanu.ac.ir

*Abstract*— **The hysteresis motor is a well-known synchronous motor that is used in special small power, high speed applications. Dynamic modeling and analysis of this motor is more complicated than permanent magnet synchronous motors (PMSMs) or induction motors (IMs) due to nonlinearity behavior of rotor magnetic material. Overexcitation is a unique phenomenon that only occurs in hysteresis motor that can be proposed as; when the terminal voltage $V_i$ of the hysteresis motor running at synchronous speed is continuously increased up to $nV_i$ ($n > 1$) and then continuously decreased to $V_i$, input currents are reduced and output power is increased at the same time. Consequently, overexcitation reduces the stator copper and enhances efficiency. Till now, there isn't any analytic dynamic model of this overexcitation. In this paper, based on a novel dynamic model of hysteresis motor, the overexcitation phenomenon is investigated and transient performance of motor is simulated via Matlab/Simulink.**

***Keywords- Hysteresis Motor; Overexcitation; Efficiency; Dynamic Modeling, B-H Loop.***

## I. INTRODUCTION

The hysteresis motor can be regarded as a self-starting synchronous machine, which has the same structure as squirrel cage asynchronous motor with exception that its rotor consist of a ring of magnetic material which covers a non-magnetic core. It is often used for small power applications that need to very smooth torque at high speed such as gas centrifuge and gyroscope [1]. Relatively low starting current, simple and strong structure, uniform torque-speed characteristic and also low power factor, low efficiency and hunting phenomenon are some of hysteresis motor advantages and disadvantages [2]. There are two main structures for hysteresis motors: cylindrical and disk types. Cylindrical hysteresis motors are classified in two types of circumferential-flux and radial-flux. In circumferential-flux hysteresis motor, the rotor ring is mounted on non-magnetic material as the support. The magnetic field lines in rotor are mostly circumferential to the ring. This type of hysteresis motor is mostly used in industrial applications [3]. Fig. 1 shows structure of a circumferential-flux hysteresis motor.

Rotors in [4] showed that overexcitation for a short period of hysteresis motor running at synchronous speed causes the reduction of stator current and the increase of pullout torque at the same time. This phenomenon is very important from the view point of high-efficiency operation and has been discussed by some researchers [5-8]. They have investigated overexcitation, but could not model this phenomenon. Lately, overexcitation has been experienced via variable frequency inverters and various voltage patterns have been applied to hysteresis motor to gain more efficient performance for hysteresis motor [9-11]. But it has not presented any dynamic model to predict the transient performance of hysteresis motor during overexcitation. This paper investigates the transient behavior of motor during short overexcitation based on a novel dynamic model for hysteresis motor. The paper is organized as follows: In section II, the overexcitation phenomenon is described briefly. Section III proposes a novel dynamic model of hysteresis motor. In section IV, some simulation results are given and then conclusion is explored in section V.

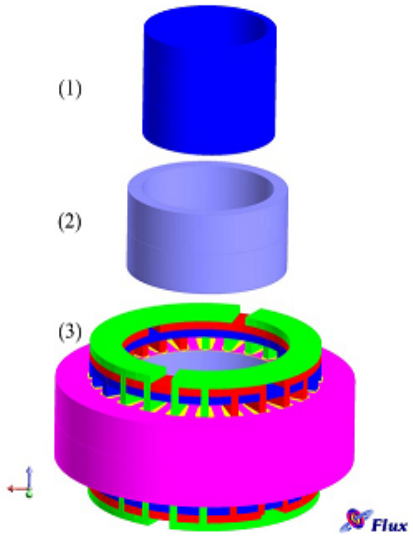


Fig. 1. Structure of circumferential-flux type of hysteresis motor
(1) Rotor support, (2) Rotor ring (3) Stator (core & windings)

## II. OVEREXCITATION PHENOMENON

Since the power factor of hysteresis motor is much lower than of an induction motor, it takes more RMS current and hence large capacity condensers are installed to improve the

power factor. However, this is not favorable because the cost increases and also the resonance is caused by presence of hysteresis motor inductance and condenser capacitance and efficiency is not improved. Short Overexcitation is an effective process for increasing output power, improving power factor and efficiency and reducing input current [12]. Overexcitation means that the input voltage $V_i$ applied to the motor operating at synchronous speed is increased continuously up to $nV_i$ ($n > 1$) and then continuously decreased up to $V_i$. Factor n is called overexcitation factor.

### *A. Terminal voltage pattern with short-duration overexcitation*

Fig. 2 shows the method for the overexcitation considered here. The motor is accelerated to synchronous speed with stator voltage $V_i$. After synchronization, stator voltage is raised to a higher value $nV_i$ for a short period, and then reduced to original value $V_i$. It is assumed that the load torque remains unchanged during this change. In this paper a circumferential-flux type hysteresis motor is analyzed, although proposed analysis can also be applied to a radial-flux type hysteresis motor.

### *B. Magnetic Behavior of Rotor Hysteresis Material before and after overexcitation*

Let us first investigate the magnetic state of the rotor before overexcitation. When the rotor turns at sub-synchronous speed, any point in the rotor hysteresis material experiences a sinusoidal variation of flux density B in time, and consequently a magnetic hysteresis loop Lo shown in Fig. 3(a). Other points in the rotor hysteresis material experience exactly the same hysteresis loop, displaced in time phase. Thus the loop not only gives the time variation of the magnetic state at a point in the rotor, but also gives the space variation of magnetic state around rotor at a particular instant of time [7,13]. The area of this loop is proportional to output torque $T_{em}$.

When the motor reaches its synchronous speed, magnetic state at any point momentarily stops changing. For example, the magnetic state at a point P in Fig. 3(b) in the rotor stops at the location of $P_0$ on the loop shown in Fig. 3(a), and the magnetic state at another point stops at $Q_0$ on the same loop. If the load torque is equal to the output torque $T_{em}$, the motor speed will not change further. But, if the load torque is less than $T_{em}$, the motor speed will increase further and a displacement of the rotor forward with respect to the rotating flux density wave will occur. So, the points of P0 and Q0

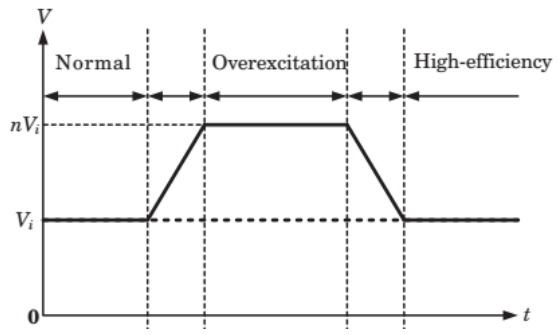


Fig. 2. Terminal voltage pattern

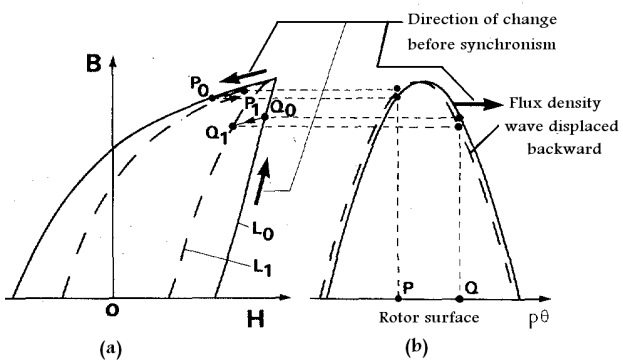


Fig. 3. B-H loops and flux density waves for two different loads [7,13]. ($L_1$ loop corresponds to the lower load)

come to $P_1$ and $Q_1$ that means the operational B-H loop goes to other loop L1. Hence, a new B-H loop is created that its area is smaller than loop $L_0$. It means that with changing load torque, the B-H loop will not be fixed. The same behavior can be explained when the load torque increases, so that loop $L_1$ will be wider than loop $L_0$. The shape of $L_1$ is different from the major hysteresis loop created by rated input voltage or from those of the minor hysteresis loops created by lower voltages. Since the area of the B-H loop is proportional to the output torque [1], the area of loop $L_1$ is proportional to output torque witch is in equilibrium with load torque.

Now, let us investigate the change in the magnetic state of the rotor when it is overexcited. When the stator voltage is increased from $V_i$ to $nV_i$, the flux density in the rotor also increases. Therefore, the points $P_1$, $Q_1$ on loop $L_1$ will ascend along their respective minor loops toward the ascending branch of the major loop $L_0$ in Fig. 4(a). The points that meet the ascending branch of loop $L_0$ will go up further along it the points that pass the tip of the major loop $L_0$ will ascend along the normal magnetization curve of the rotor hysteresis material.

For example, the points $P_1$, $Q_1$ will come to $P_2$, $Q_2$, respectively. Thus, the B-H relation around the rotor is given by a closed loop $L_2$ in Fig. 4(a). It should be noted that load torque remains unchanged during mentioned process. This means that the area of loop $L_2$ must be equal to that of loop $L_1$. In other words, the amplitude and the phase of the flux density distribution in the rotor are such that the areas of both loops

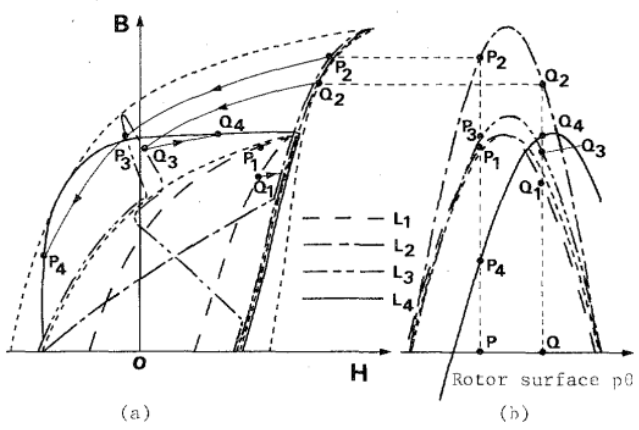


Fig. 4. B-H loops and flux density waves during overexcitation process [7].

are equal. Such flux density distribution and therefore loop $L_2$, can be obtained from an iterative calculation. When stator voltage is reduced from $nV_i$ to original value $V_i$, the flux density in rotor now decreases. Therefore, for example, points $P_2$ and $Q_2$ on loop $L_2$ descend along the descending branch of the respective major loops whose tips are $P_2$ and $Q_2$, and come to $P_3$ and $Q_3$, respectively, as shown in Fig. 4(a). Thus, the B-H relation around the rotor is given by a closed loop $L_3$. The area of loop $L_3$ must be equal to that of loop $L_2$, because the load torque is constant. If the load torque is increased, there will be a decrease of speed and a displacement of the rotor backward with respect to the rotating flux. Then, for example, the flux density at point P decreases to P4 and the flux density at point Q increase to Q4 as shown in Fig. 4(b). As a result, the B-H relation given by loop $L_4$ in Fig. 4(a) can be obtained, the area of which is corresponding to the pull-out torque after overexcitation [7].

## III. Dynamic Model of Hysteresis Motor

The common point in all mentioned steady-state equivalent circuit models is that the rotor's hysteresis loop is considered as hysteresis resistance $R_h$ in series with reactance $X_h$ in sub synchronous mode as shown in Fig. 5 [13]. In this section a new dynamic model for hysteresis motor with incorporating the change of load torque and stator voltage to identify the operational B-H loop of the rotor is developed [14].

### *A. Calculation of Rotor's Equivalent Circuit Parameters*

Hysteresis motor used in this paper is a high speed circumferential-flux type motor, 3-phases, star-connected, with given parameters in Table I. To develop dynamic model of hysteresis motor, the value of rotor's parameters due to operational hysteresis motor must be calculated. For this purpose B-H curves of rotor material are firstly measured by some standard experiments. Employed magnetic material used in this study is Vicalloy 2 with typical B-H loops shown in Fig. 6 [15]. It is a composition of Vanadium-Iron-Cobalt. Maximum achieved output hysteresis torque in steady state is corresponding to maximum applied voltage to stator that is proportional to major hysteresis loop. For simplicity of calculation, the fundamental harmonic of magnetic field intensity ($H$) and field density ($B$) are just considered. In other words, the hysteresis loops are considered elliptical.

The flowchart for calculation of the motor's parameters in air gap and rotor circuit is shown in Fig. 7 [14,16]. Firstly, the operational B-H loop or corresponding lag angle $\beta$ due to applied stator voltage $V_{in}$ is identified and then is modified based on applied load torque using equivalent circuit shown in Fig. 5. In this circuit, $R_s + jX_{ls}$ is stator leakage impedance, $R_c \| jX_m$ is air gap impedance, and $(R_h + jX_h) \| R_e / s$ is equivalent rotor impedance. The air gap reactance and rotor impedance are expressed as [16]:

$$X_m = \frac{2m\omega\left(K_w N_{ph}\right)^2 \mu_0 r_g l_h}{\pi P^2 g} \tag{1}$$

$$R_h = \frac{m\omega\left(K_w N_{ph}\right)^2 \mu V_r}{\pi^2 r_h^2} \sin\beta \tag{2}$$

$$X_h = \frac{m\omega\left(K_w N_{ph}\right)^2 \mu V_r}{\pi^2 r_h^2} \cos\beta \tag{3}$$

As mentioned earlier, when the hysteresis motor reaches synchronous speed, developed torque $T_{em}$ is equal to load torque $T_l$. The steady-state developed torque in terms of hysteresis ring's volume, operational B-H loop properties and

TABLE I
RATED SPECIFICATIONS AND PARAMETERS OF TYPICAL CIRCUMFERENTIAL-FLUX HYSTERESIS MOTOR

| Symbol | Quantity | Value | Dimension |
|---|---|---|---|
| $V_{rated}$ | line rated voltage | 230 | V |
| $T_{rated}$ | rated torque | 0.01 | N.m |
| $f_{rated}$ | rated frequency | 100 | Hz |
| $\omega$ | supply angular frequency | $2\pi\times100$ | rad/sec |
| $m$ | number of phase | 3 | |
| $P$ | number of poles | 2 | |
| $J$ | shaft inertia moment | $3\times10^{-4}$ | kg.m$^2$ |
| $R_s$ | stator resistance | 60 | Ω/ph |
| $R_c$ | stator core loss equivalent resistance | 10580 | Ω/ph |
| $R_h$ | rated rotor hysteresis resistance | 300 | Ω/ph |
| $R_e$ | eddy current resistance of rotor | 223 | Ω/ph |
| $X_{ls}$ | stator leakage reactance | 78 | Ω/ph |
| $X_m$ | rated magnetizing reactance | 400 | Ω/ph |
| $X_h$ | rated rotor hysteresis reactance | 170 | Ω/ph |
| $l_h$ | axial length of hysteresis ring | 25 | mm |
| $g$ | air gap length | 1 | mm |
| $t_r$ | thickness of hysteresis ring | 1 | mm |
| $\beta$ | hysteresis lag angle | 60° | |

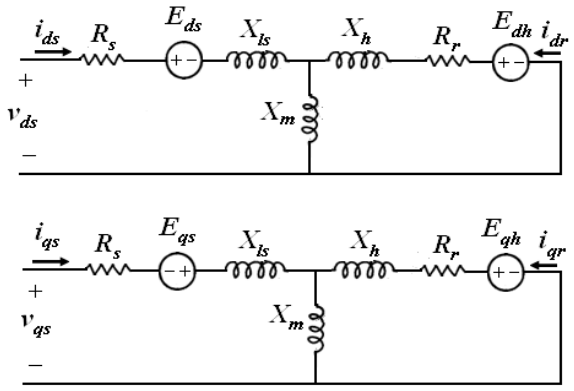


Fig. 5. Equivalent circuit for dynamic model of hysteresis motor in rotating dq reference frame

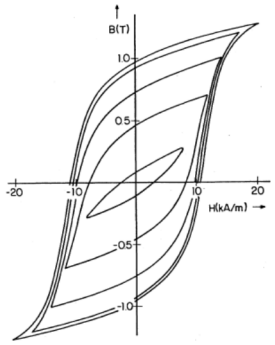


Fig. 6. B-H characteristics for a typical Vicalloy magnetic material used in hysteresis motor [15]

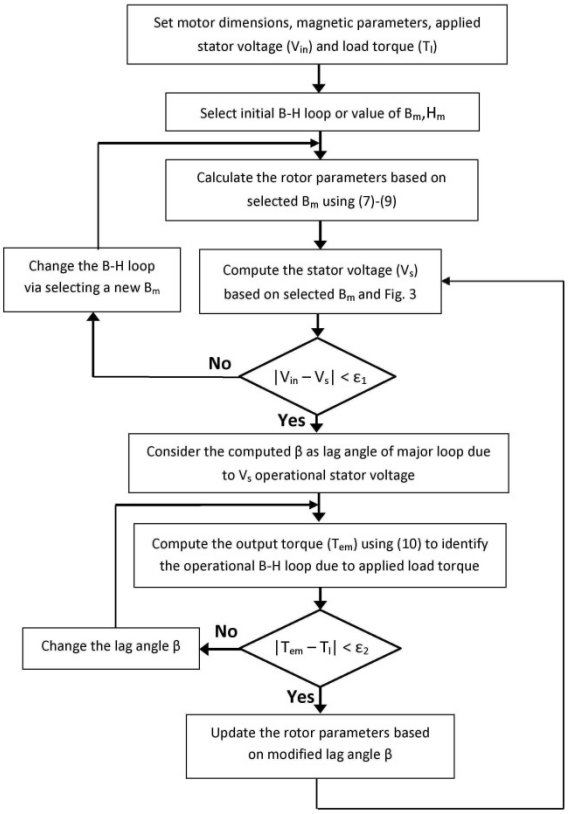


Fig. 7. Flowchart for calculation of the rotor's equivalent circuit parameters [16]

lag angle $\beta$ can be expressed as [17]:

$$T_{em} = \frac{mP}{2}\pi(B_m H_c) r_h t_r l_h \sin\beta \tag{4}$$

It means that if under constant stator voltage, the load torque varies, operational B-H loop changes without changing value of $B_m$ and $H_m$ and so the lag angle $\beta$ varies as shown in Fig. 3. Therefore, in final stage of computation, developed torque $T_{em}$ through (4) is compared with the load torque and lag angle $\beta$ is iterated by a proper step size until the torque difference falls to desired tolerance $\varepsilon_2 = 0.0005\ N.m$ as shown in Fig. 7.

Hysteresis motors use the semi-hard magnetic materials that unlike to induction motors induce considerable back-EMF voltage in stator. For dynamic modeling of hysteresis motor, we consider an induced voltage source in the rotor circuit. This equivalent induced voltage $E_h$ for hysteresis material can be obtained from induced voltage at synchronous speed in steady-state model:

$$\vec{E}_h = \sqrt{\left(X_m I_s \sin\theta_g + (X_h + X_m) I_h \sin\beta\right)^2 + \left(X_m I_s \cos\theta_g + (X_h + X_m) I_h \cos\beta\right)^2} \angle -\theta_h \tag{5}$$

where

$$\theta_h = \tan^{-1}\left(\frac{X_m I_s \cos\theta_g + (X_h + X_m) I_h \cos\beta}{X_m I_s \sin\theta_g + (X_h + X_m) I_h \sin\beta}\right) \tag{6}$$

Calculated $E_h$ is a phasor corresponding to phase 'a'. It has to be expressed in time domain for three phases and then transferred to $E_{dh}$ and $E_{qh}$ in dq reference frame.

### *B. Mathematical Model and Equivalent Circuit of Hysteresis Motor in Rotating dq Reference Frame*

The hysteresis motor voltage equations in synchronously rotating dq reference frame can be written as:

$$V_{dq} = R \cdot I_{dq} + \frac{d\Lambda_{dq}}{dt} + E_{dq} \tag{7}$$

where,

$$V_{dq} = \begin{bmatrix} v_{ds} \\ v_{qs} \\ v_{dr} = 0 \\ v_{qr} = 0 \end{bmatrix}, I_{dq} = \begin{bmatrix} i_{ds} \\ i_{qs} \\ i_{dr} \\ i_{qr} \end{bmatrix}, \Lambda_{dq} = \begin{bmatrix} \lambda_{ds} \\ \lambda_{qs} \\ \lambda_{dr} \\ \lambda_{qr} \end{bmatrix}, E_{dq} = \begin{bmatrix} E_{ds} \\ E_{qs} \\ E_{dh} \\ E_{qh} \end{bmatrix} \tag{8}$$

where the rotor resistance is calculated from:

$$R_r = \frac{1}{1/R_h + s/R_e} \tag{9}$$

The foregoing equations can be summarized in the equivalent circuit model as shown in Fig. 5.

## IV. Simulation Results

Simulated for a true hysteresis motor with summarized parameters in table I. Simulations are carried out in various conditions: variable overexcitation factor, variable terminal voltage pattern. The predominant load of employed hysteresis motor is rotational friction as $T_l = B_f \cdot \omega_m^2$ that the value of $B_f$ is 1 in per unit scale. Fig. 8 shows the current and power factor of motor for overexcitation factor (n=1.25). It is seen that the input current decreases after reduction input voltage from 0.19 A to 0.13 A. It means the cupper loss of stator reduces 4 times than before overexcitation. On the other hand, power factor increases from 0.54 to 0.77 that means a 50% increment. Fig. 9 shows the variations of lag angle β and rotor's impedance components due to hysteresis material of the rotor. During overexcitation, lag angle decreases and then it increases. The variations of $R_h$ and $X_h$ obey (2)-(3).

Fig. 10 shows the current and power factor of motor for n=1.1. Fig. 11 shows the different terminal voltage pattern with current and power factor. RMS of current decreases form 0.19 A to 0.16 A, and the power factor increases from 0.54 to

0.64. Comparing of the results shown in Fig. 8 and Fig. 11 proves that the larger increase of terminal voltage pattern leads to better performance and higher power factor and efficiency. Using developed dynamic model of hysteresis motor, it is possible to predict the best choice for order "n" for overexcitation process.

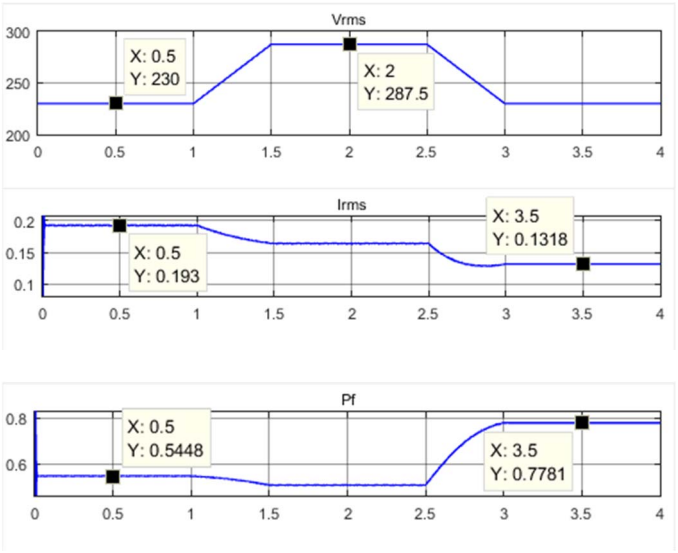


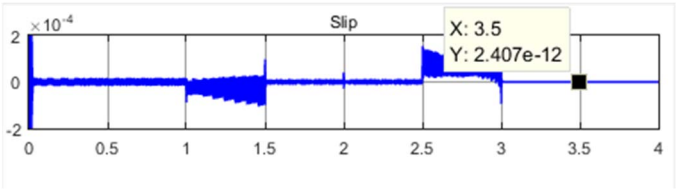


Fig. 8. Input voltage, current, power factor, slip before and after overexcitation (n=1.25)

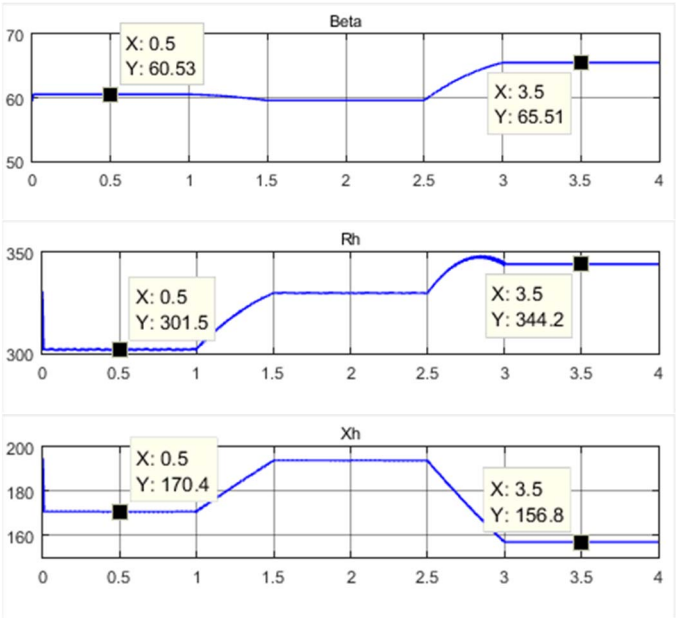


Fig. 9. Lag angle β, $R_h$ and $X_h$ before and after overexcitation (n=1.25)

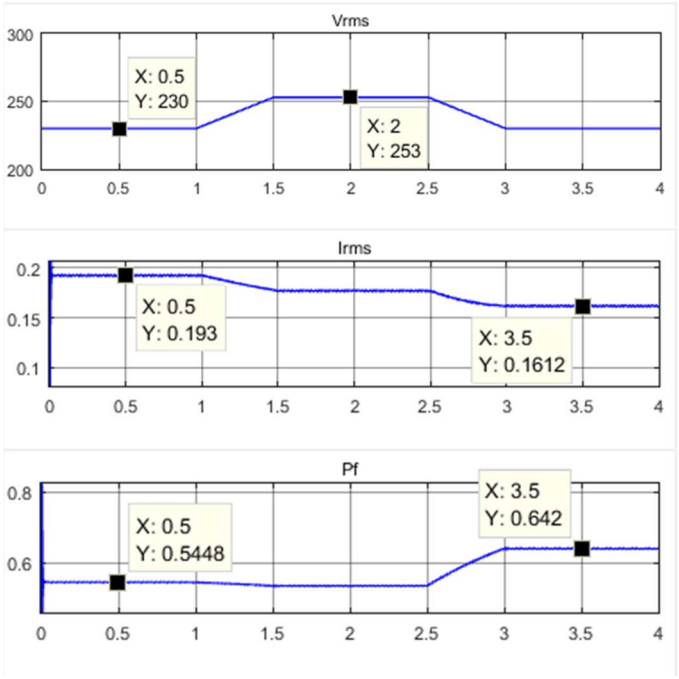


Fig. 10. Input voltage, current, power factor before and after overexcitation (n=1.1)

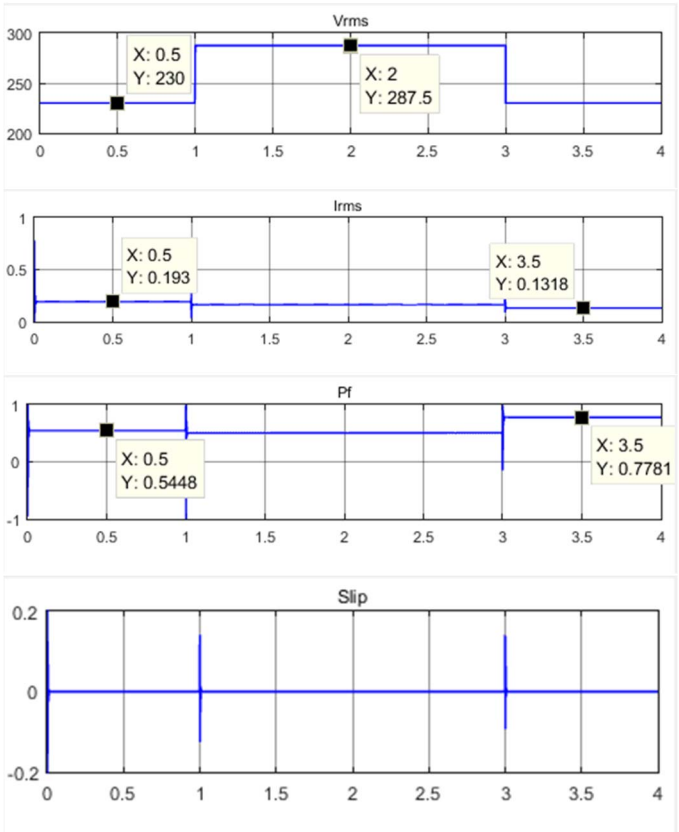


Fig. 11. Input voltage, current, power factor, slip before and after overexcitation (n=1.25)

## V. CONCLUSIONS

Short duration overexcitation increases the efficiency, power factor and pull-out torque of hysteresis motor and makes it possible to operate in efficient condition. Determination of voltage amplitude and time duration in overexcitation process is essential to attain the best operational point. In this paper, the short overexcitation phenomenon of a hysteresis motor has been modeled and simulated for the first time. On this way, a novel dynamic model of hysteresis motor in rotation dq reference frame was presented. In developed model, the operational B-H curve of the motor is considered during change of input voltage or load torque. Simulation results show the effectiveness of developed model to predict the motor performance during overexcitation. By using developed model it is possible to evaluate the effect of motor parameters, B-H characteristics of rotor material, magnitude of input voltage, time duration and acceleration/deceleration of voltage variations during short-overexcitation process.

## REFERENCES


[1] B.R. Teare, "Theory of Hysteresis Motor Torque", AIEE Transactions, vol. 59, pp. 907-912, 1940.

[2] M.A. Copeland and G.R. Slemon, "An Analysis of the Hysteresis Motor: part-I-Analysis of the Idealized Machine", IEEE Trans. on Power Apparatus and System, vol. 82, no. 65, pp. 34-42, 1963.

[3] M.A. Copeland and G.R. Slemon, "An Analysis of the Hysteresis Motor: part-II-The Circumferential-flux Machine", IEEE Trans. on Power Apparatus and Systems, vol. 83, pp. 619-625, June 1964.

[4] H. C. Rotors, "The hysteresis motor-advances which permit economical fractional horsepower ratings," AIEE Trans., vol. 66, pp. 1419-1430, 1947.

[5] D. O'Kelly, "Hysteresis motor with overexicitation and solid state control," IEE Proc., vol. 120, pp. 1533-1537, 1973.

[6] G. Wakui and S. Nishino, "Performance of hysteresis motor after shortduration overexicitation (underexicitation) and its analysis," Trans. Inst. Elect. Eng. Japan, vol. 101, pp. 347-354, 1981.

[7] T. Kataoka, T. Ishikawa, and T. Takahashi, "Analysis of a hysteresis motor with overexicitation," IEEE Trans. on Magnetics, vol. 18, pp. 1731-1733, 1982.

[8] T. Ishikawa and T. Kataoka, "V curve of hysteresis motor," IEE Proc. B, vol. 138, pp. 137-141, 1991.

[9] G. Wakui, I. Ohahi and K. Kurihara; "Automatic Operation of Hysteresis Motor with Short Duration Overexcitation", Electrical Engineering in Japan, vol. 103, no. 6, 1983, pp. 98-105.

[10] T. Kubota, K. Kurihara, and T. Tamura; "Characteristics of PWM inverter-driven hysteresis motor with short-duration overexcitation", International Conference on Electrical Machines and Systems (ICEMS), 2010, 1429-1433.

[11] T. Kubota, T. Tamura, and K. Kurihara; "New Scheme for High-Efficiency Operation of PWM Inverter-Driven Hysteresis Motor with Short-Duration Overexcitation", XIX International Conference on Electrical Machines (ICEM), 2010, pp. 1-6.

[12] T. Kubota, T. Tamura and K. Kurihara; "High-Efficiency operation of PWM inverter-driven hysteresis motor with short-duration overexcitation," International Conference on Electrical Machines and Systems, (ICEMS 2009), 2009, pp. 1-4.

[13] A. Halvaei Niasar, A. Ghanbari; "Evaluation of Various Dynamic Modeling Methods of a Circumferential-Flux Hysteresis Motors", in Proceedings of the 7th Power Electronics, Drive Systems & Technologies Conference (PEDSTC), 2016.

[14] A. Halvaei Niasar, A. Ghanbari, A. PirZadeh; "An Improved Analytical Dynamic Modeling of Hysteresis Motor", in Proceedings of the 24th Iranian Conference on Electrical Engineering (ICEE), May 10-12, 2016.

[15] R.D. Jackson, M.A. Rahman, and G.R. Slemon; "Analysis and Determination of Ring Flux Distribution in Hysteresis Motors", IEEE Trans. on Power Apparatus and Systems, vol. PAS-102, no. 8, pp. 2743-2749, August 1983.

[16] A. Halvaei Niasar; "A Novel Time Varying Dynamic Modeling for Hysteresis Motor," Journal of Scientia Iranica, Sharif University of Technology, 2016, (in Press).

[17] M.A. Rahman and A.M. Osheiba;, "Dynamic Performance Prediction of Poly Phase Hysteresis Motors", IEEE Trans. on Industry Applications, vol. 26, no.6, pp. 1026-1033, 1990.